NASA/TM-20240001961

Metallurgical and Thermal Properties of 57Ni-40Ti-3Hf (wt%)

Malcolm K. Stanford
Glenn Research Center, Cleveland, Ohio

March 2024

NASA STI Program Report Series

Since its founding, NASA has been dedicated to the advancement of aeronautics and space science. The NASA scientific and technical information (STI) program plays a key part in helping NASA maintain this important role.

The NASA STI program operates under the auspices of the Agency Chief Information Officer. It collects, organizes, provides for archiving, and disseminates NASA's STI. The NASA STI program provides access to the NTRS Registered and its public interface, the NASA Technical Reports Server, thus providing one of the largest collections of aeronautical and space science STI in the world. Results are published in both non-NASA channels and by NASA in the NASA STI Report Series, which includes the following report types:

- TECHNICAL PUBLICATION.
  Reports of completed research or a major significant phase of research that present the results of NASA Programs and include extensive data or theoretical analysis. Includes compilations of significant scientific and technical data and information deemed to be of continuing reference value. NASA counterpart of peer-reviewed formal professional papers but has less stringent limitations on manuscript length and extent of graphic presentations.

- TECHNICAL MEMORANDUM.
  Scientific and technical findings that are preliminary or of specialized interest, e.g., quick release reports, working papers, and bibliographies that contain minimal annotation. Does not contain extensive analysis.

- CONTRACTOR REPORT.
  Scientific and technical findings by NASA-sponsored contractors and grantees.

- CONTRACTOR REPORT.
  Scientific and technical findings by NASA-sponsored contractors and grantees.

- CONFERENCE PUBLICATION.
  Collected papers from scientific and technical conferences, symposia, seminars, or other meetings sponsored or co-sponsored by NASA.

- SPECIAL PUBLICATION.
  Scientific, technical, or historical information from NASA programs, projects, and missions, often concerned with subjects having substantial public interest.

- TECHNICAL TRANSLATION.
  English-language translations of foreign scientific and technical material pertinent to NASA's mission.

Specialized services also include organizing and publishing research results, distributing specialized research announcements and feeds, providing information desk and personal search support, and enabling data exchange services.

For more information about the NASA STI program, see the following:

- Access the NASA STI program home page at http://www.sti.nasa.gov

NASA/TM-20240001961

Metallurgical and Thermal Properties of 57Ni-40Ti-3Hf (wt%)

Malcolm K. Stanford
Glenn Research Center, Cleveland, Ohio

National Aeronautics and
Space Administration

Glenn Research Center
Cleveland, Ohio 44135

March 2024

Acknowledgments

This work was made possible by the superb technical assistance from Joy A. Buehler, C. Crochet, Drew J. Davidson, Thomas Goerz, Dereck F. Johnson, Robert Larsen, Richard E. Martin, Ralph J. Pawlik and Henry N. Scott and the helpful discussions with Dr. Othmane Benafan. This work was funded by NASA's Transformational Tools and Technologies Project.

NASA STI Program/Mail Stop 050
NASA Langley Research Center
Hampton, VA 23681-2199

Metallurgical and Thermal Properties of 57Ni-40Ti-3Hf (wt%)

Malcolm K. Stanford
National Aeronautics and Space Administration
Glenn Research Center
Cleveland, Ohio 44135

Abstract

Selected properties of 57Ni-40Ti-3Hf (wt%) were measured to further develop this material for use in aerospace rolling-element bearings. The average grain size and microindentation hardness of the material at room temperature were 90 μm and 549 HV, respectively. From room temperature to 500 °C, electrical resistivity increased from 8.9×10^{-7} to 11.3×10^{-7} Ω·m, thermal expansion coefficients varied from 1.1×10^{-5} to 1.2×10^{-5} mm/mm·°C, specific heat increased from 0.44 to 0.53 W·sec/g·K, thermal diffusivity rose from approximately 0.003 to 0.005 cm^2/sec and thermal conductivity increased from approximately 0.09 to 0.19 W/cm·K. The behavior of the material can be explained by well-known metallurgical theory. These results are expected to provide a basis for design and modeling of future aerospace components.

Background

57Ni-40Ti-3Hf (wt%) is a material developed by NASA for use in rolling-element bearings (Refs. 1 and 2). This material is a modification of 60-Nitinol (60Ni-40Ti (wt%)), having high-hardness, low apparent elastic modulus and superior resistance to aqueous corrosion, with the hafnium serving to reduce the temperature necessary to harden the material (Ref. 3). Due to its unique combination of properties, 57Ni-40Ti-3Hf is more resilient to transient overloads and to the marine air environment that exists at U.S. spaceports, shipyards, and coastal airfields. There are several possible aerospace components that could be developed for future applications. However, thermophysical properties of 57Ni-40Ti-3Hf are needed to develop accurate models of components. The purpose of this study is to measure selected thermophysical properties of 57Ni-40Ti-3Hf to improve design and modeling of future components.

In previous work, thermophysical properties of 60-Nitinol were reported (Ref. 4). These properties are not expected to vary greatly for 57Ni-40Ti-3Hf due to compositional similarity. However, this study is necessary for completeness and to improve accuracy of design and modeling of critical components. Some properties have been found to follow estimates based on the Rule of Mixtures. Since this may be a viable alternative for some screening studies, this topic will be addressed in the Appendix.

Test Methods

57Ni-40Ti-3Hf (wt%), hereafter referred to as Ni-Ti-Hf, was fabricated in powder form by electrode inert gas atomization. Properties of the powder are shown in Table I. The powder was then consolidated into ingots by hot isostatic pressing (HIP) by a commercial source (Ref. 5). The HIP cycle was 980±25 °C at 103±3 MPa for 4 h +0.25/–0.0 h followed by furnace cooling. The composition of the consolidated material is given in Table II. Specimens were sectioned by wire electrical discharge machining from two separate ingots, labeled C3520-3 and C3520-4. Specimens were heat treated by homogenizing under argon at 1050 °C for 48 h followed by furnace cooling. The specimens were then heat treated by hardening at 900 °C under argon for 2 h followed by water-quenching and then aging at 400 °C for

TABLE I.—PROPERTIES OF PRE-COMPACTION Ni-Ti-Hf POWDER

Sieve designation[a]	+200/–100
Flow time for 50 g[b]	4.6±0.7 sec
Apparent density[c]	4.07 g/cm^3
Tap density[d]	4.90/cm^3

[a]ASTM B214, "Standard Test Method for Sieve Analysis of Metal Powders," ASTM Standards, 2022, vol. 02.05, American Society for Testing and Materials, West Conshohocken, PA.
[b]ASTM B964, "Standard Test Methods for Flow Rate of Metal Powders Using the Carney Funnel," ASTM Standards, 2016, vol. 02.05, American Society for Testing and Materials, West Conshohocken, PA.
[c]ASTM B212, "Standard Test Method for Apparent Density of Free-Flowing Metal Powders Using the Hall Flowmeter Funnel," 2021, vol. 02.05, American Society for Testing and Materials, West Conshohocken, PA.
[d]ASTM B527, "Standard Test Method for Tap Density of Metal Powders and Compounds," 2022, vol. 02.05, American Society for Testing and Materials, West Conshohocken, PA.

TABLE II.—COMPOSITION OF COMPACTED Ni-Ti-Hf POWDER

----------	Ingot C3520-3	Ingot C3520-4
Composition, wt%	57.6 Ni-39.0 Ti-3.42 Hf	57.3 Ni-39.3 Ti-3.42 Hf
Impurities, ppm	O (457), N (24), C (109)	O (442), N (15), C (102)

30 min followed by water quenching. Heat treatments of this material are typically carried out under vacuum but because the vacuum furnace was undergoing repairs, these heat treatments were conducted in argon.

After heat treatment, cylindrical specimens approximately 12 mm in diameter were prepared for metallographic examination while specimens for thermophysical testing were surface ground to achieve dimensional tolerances and to remove surface oxides. The coefficient of thermal expansion, specific heat, thermal diffusivity, thermal conductivity, and electrical resistivity of hardened Ni-Ti-Hf specimens were measured from room temperature to 500 °C by a commercial source.[1] The test temperature range was selected based on anticipated service temperatures for this material. The evaluation methods are described below.

The porosity was measured using an optical microscope equipped with commercially available image analysis software in 24-bit color. The software was calibrated so that each pixel corresponded to approximately 177 nm in both the horizontal and vertical directions. Thresholding was selected from 88 to 255 to count the reflective (non-pore) area of the material. Grain size of the studied material after heat treatment was measured using the planimetric method (Ref. 6). A total of six specimens were taken from the top, middle, and bottom of the two ingots. A circle approximately 120,000 μm^2 was superimposed on each optical image that was captured at 100× magnification so that the number of grains within the circle and intersecting the circle could be counted manually. Fifteen measurements were taken from each specimen and the average value of the equivalent diameter was reported. Overall imaging of the microstructure was done using a field-effect scanning electron microscope (SEM).

Microindentation hardness, the resistance of the material to penetration by a pyramidal diamond Vickers indenter, was measured based on a standard test method (Ref. 7). A load of 200 gf (≈1.96 N) was used with an indentation spacing of 0.1 mm. Ten measurements were taken from each of three representative hardened specimens and the average hardness value was reported.

[1]Thermophysical Properties Research Laboratories, Inc. (West Lafayette, IN).

Electrical Resistivity

Electrical resistivity, the resistance a material imposes to the flow of electrons, was measured using the four-point probe technique (Ref. 8). In this method, four probes are aligned and affixed to a face of an approximately 57 by 9 by 9 mm (2.25 by 0.35 by 0.35 in.) specimen. The two outer probes supply a current, while the two inner probes measure the resistance to that current along a specified length between the inner probes. The test was performed in argon gas using a heating and cooling rate of 2 °C per minute. The change in specimen length with respect to temperature was not accounted for in this measurement.

Coefficient of Thermal Expansion

For most materials, an increase in heat input causes the vibrational amplitude of its atoms to increase such that their effective atomic radii increase. This results in the expansion in material volume. For isotropic materials, this expansion is the same in the three orthogonal directions and the expansion in one of these directions is often used for basic comparisons. This method is used here with the assumption that the studied multiphase material is isotropic.

Two specimens measuring approximately 51 by 6.35 by 6.35 mm (2.00±0.005 by 0.25 by 0.25 in.) were machined. The linear coefficient of thermal expansion α for each specimen is determined by measuring the relative change in length $\Delta L/L$ with respect to the change in test temperature by the following relationship:

$$\alpha = \frac{\Delta L}{L} \Big/ (T - T_0) \tag{1}$$

where T is the test temperature and T_0 is room temperature. Measurement of thermal expansion was performed in a helium atmosphere using a dual push-rod dilatometer at a heating rate of 2 °C per minute based on a standardized test method (Ref. 9). The instrument was calibrated using six reference materials with a range of expansion coefficients, which were obtained from the National Institute of Standards (NIST).

Specific Heat

Specific heat c_p is the energy required to increase the temperature of a gram of material by one degree at constant pressure. The specific heat of the studied material was measured in argon with a differential scanning calorimeter using a sapphire reference material according to a standard test method (Ref. 10). The test exposes an approximately 5.8 mm diameter by 1.5 mm thick (0.23 in. diameter by 0.06 in. thick) Ni-Ti-Hf specimen and the reference material (with known specific heat) to the same heat flux. The difference in power needed to heat both materials at the same rate is used to determine the specific heat of the studied material.

Density, Thermal Diffusivity, and Thermal Conductivity

Thermal diffusivity D is the rate at which heat flows through a material. The laser flash method was used to determine thermal diffusivity in vacuum (Ref. 11). With this method, the front face of an approximately 12.7 mm diameter by 2.5 mm thick (1/2 in. diameter by 0.1 in. thick) disk was heated by a laser pulse and the rise in temperature at the back face was recorded. Calculating the bulk density ρ of each specimen, determined using their mass and geometry, thermal conductivity κ was calculated using the following relationship:

$$\kappa = \rho c_p D \tag{2}$$

where c_p is the specific heat at constant pressure. The reader should recall here that, since density ρ is a function of temperature T, and this temperature dependence is not accounted for in this study, the effect of density on properties like thermal conductivity will not be accounted for in this study.

Results

SEM micrographs of the microstructure of the studied Ni-Ti-Hf alloy are shown in Figure 1. Though not the subject of this investigation, the parent phase has been identified as Ni-Ti-Hf and secondary phases have been identified as Ni_4Ti_3 and small amounts of HfO_2 (Ref. 12). Porosity was approximately 0.2 percent. The average equivalent grain size was approximately 90 μm. There was some variability in the grain size results from location to location on each specimen, likely due to variations in the etching rate across the surface of the specimens. The average Vickers hardness was 549±18.5 HV.

Electrical Resistivity

Electrical resistivity increased monotonically from room temperature to 500 °C for both specimens, as shown in Figure 2. This trend is expected for metals according to Bloch-Grüneisen model of resistivity with respect to temperature (Ref. 13). The reader may note that this report has avoided characterizing this data trend (or any of the trends discussed previously) as “linear,” though they appear to be so over the studied temperature range. This is because a rigorous statistical analysis of the data would need to be performed to determine the form of the best fitting curve. Moreover, Bloch-Grüneisen resistivity predicts cubic proportionality to temperature, so it is possible that temperature dependence merely appears to be linear because the studied temperature range is too narrow to show the overall trend. Nevertheless, the electrical resistivity for the studied specimens has the same order of magnitude of typical engineering metals (10^{-7} Ω·m).

To provide some context, the thermophysical properties of Ni-Ti-Hf are compared to those of other engineered bearing materials in Table III. Because the microstructures of intermetallic materials like Ni-Ti-Hf tend to contain higher densities of imperfections (e.g., point, line and area defects) compared to conventional alloys, these imperfections tend to scatter electron waves, increasing resistivity as described by Matthiessen’s rule (Ref. 14). This may explain the relatively high electrical resistivity of the studied material.

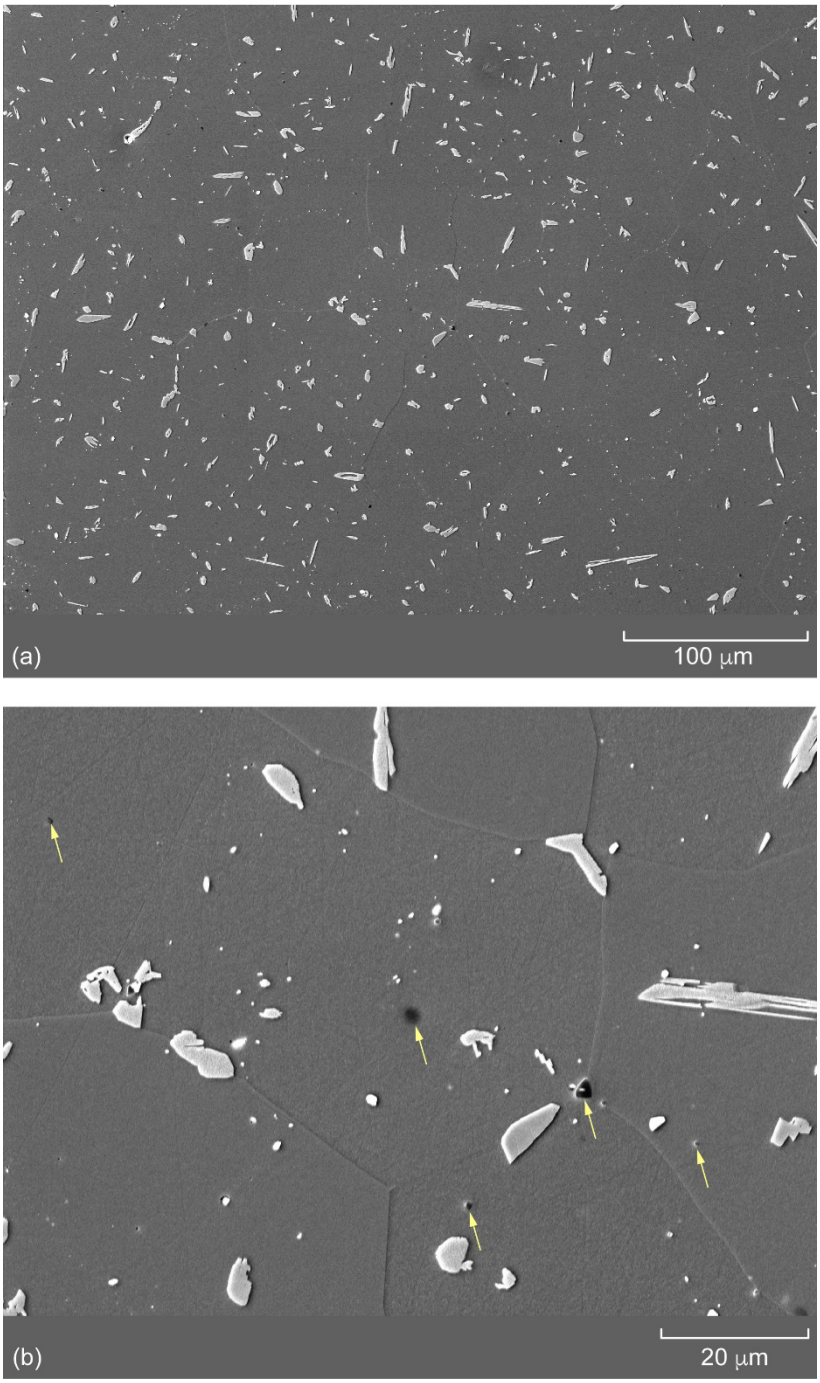

Figure 1.—SEM micrographs at (a) low- and (b) high-magnification showing the parent phase (grey) and secondary phases (light grey) in the studied alloy. Pores are visible in the microstructure, as indicated with arrows.

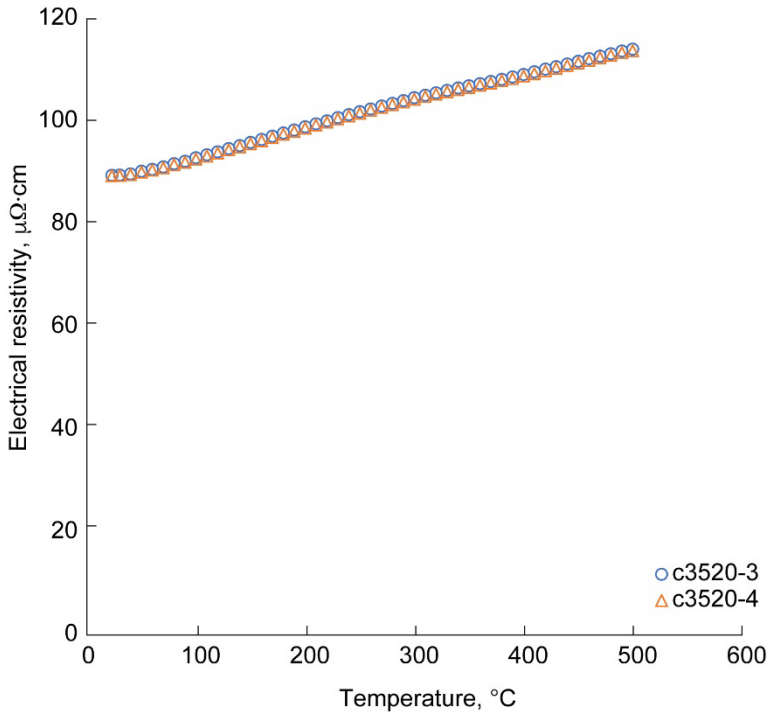

Figure 2.—Electrical resistivity.

TABLE III.—THERMOPHYSICAL PROPERTIES OF SELECTED ENGINEERED BEARING MATERIALS
[At room temperature except where noted.]

Material	Electrical resistivity, Ω·m	Linear coefficient of thermal expansion, 10^{-6}/°C	Thermal conductivity, W/m·K	Specific heat capacity, J/kg·K
Cobalt	6.2×10^{-8}	13.1 (RT-200 °C)	69 (RT-100 °C)	414 (RT-100 °C)
Nickel	8.0×10^{-8}	13.9 (RT-200 °C)	92 (RT-100 °C)	440 (RT-100 °C)
M50 (bearing steel)	1.8×10^{-7}	12.1 (RT-260 °C)	25.9 (RT-100 °C)	462 (RT-100 °C)
Titanium	4.2×10^{-7}	9.5 (RT-300 °C)	22 (RT-100 °C)	519 (RT-100 °C)
440C stainless steel	6.0×10^{-7}	10.8 (0-315 °C)	41.9 (RT-150 °C)	460 (0-100 °C)
304 stainless steel	7.2×10^{-7}	17 (RT-300 °C)	15.1 (RT-100 °C)	500 (0-100 °C)
Ni-Ti-Hf	8.95×10^{-7}	11.3 (RT-300 °C)	9.8 (RT-100 °C)	452 (RT-100 °C)
60-Nitinol	9.63×10^{-7}	11.2 (20-200 °C)	9.4 (50-100 °C)	462 (RT-100 °C)

Coefficient of Thermal Expansion

A plot of thermal expansion coefficients for the studied specimens is shown in Figure 3. The value rises from approximately 1.1×10^{-5} to 1.2×10^{-5} mm/mm·°C over the studied temperature range. Other than a minor difference of less than 5 percent at room temperature, thermal expansion for the two specimens is essentially the same throughout the studied temperature range.

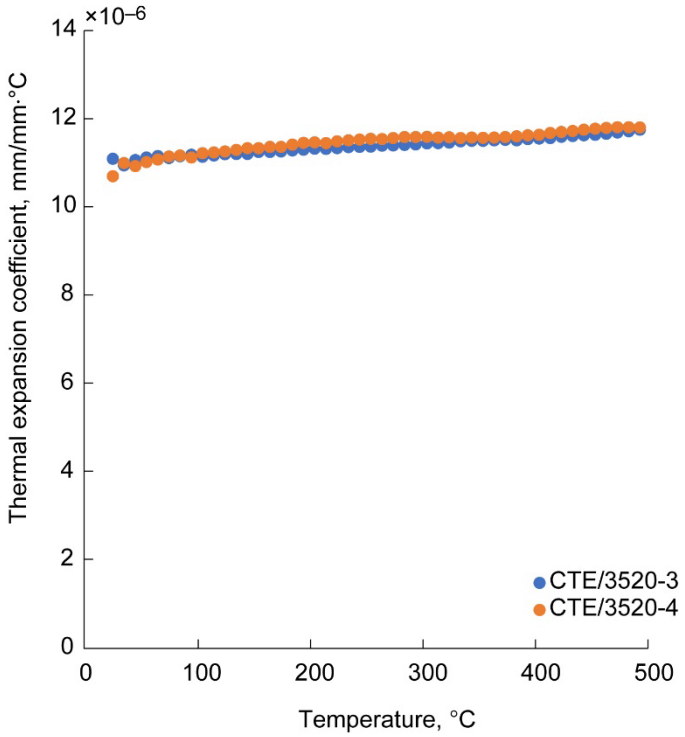

Figure 3.—Coefficient of thermal expansion for the two specimens.

Specific Heat

Figure 4 is a plot of specific heat for the two specimens from room temperature to 500 °C. The plots increase monotonically from approximately 0.44 to 0.53 W·sec/g·K. However, at approximately 400 °C the rate of change increases noticeably. The vertical axis is truncated to only show the range from approximately 0.44 to 0.54 W·sec/g·K so the rate of change in this plot is more pronounced in Figure 5. This “knee” is likely due to the formation of a precipitation phase similar to what was documented in the binary NiTi alloy (Ref. 4).

Density, Thermal Diffusivity, and Thermal Conductivity

The average density for the studied specimens was 6.75±0.03 g/cm^3. The thermal diffusivity, plotted in Figure 6, rose monotonically from approximately 0.003 to 0.005 cm^2/sec as temperature was increased from room temperature to 500 °C and was essentially the same for each specimen. As shown in Figure 7, thermal conductivity also rises with temperature, in agreement with the relationship given in Equation (2). The studied material has a significantly lower thermal conductivity than conventional engineering alloys, which can be observed in Table III. The Wiedmann-Franz law states that electrons can transfer heat through a material as well as phonons (Ref. 15). Therefore, we might expect that a material with higher electrical resistivity (i.e., lower electrical conductivity) would also have lower thermal conductivity due to the reduced availability of electrons to conduct heat. This may at least partially explain the relatively low thermal conductivity of Ni-Ti-Hf.

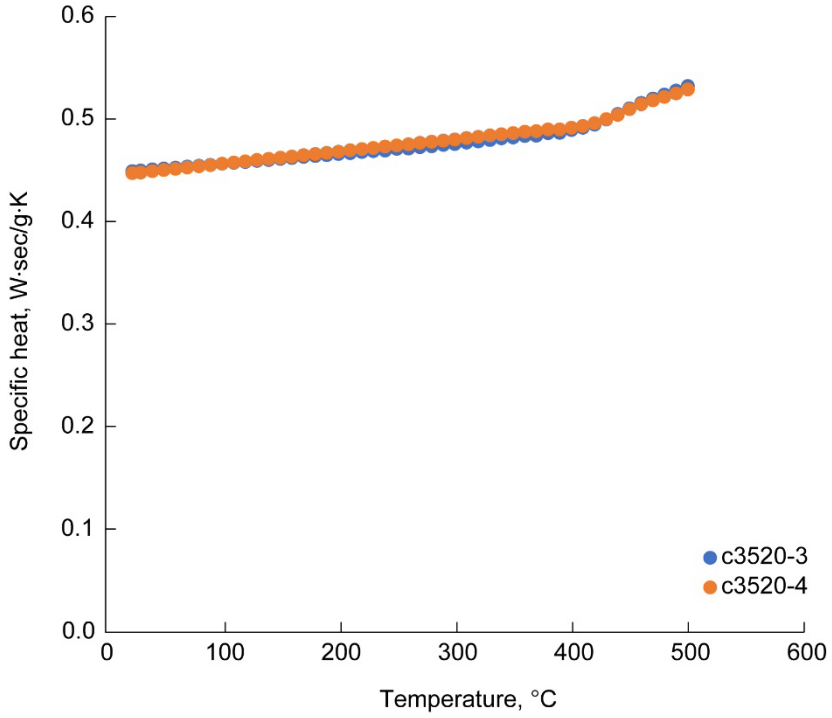

Figure 4.—Specific heat.

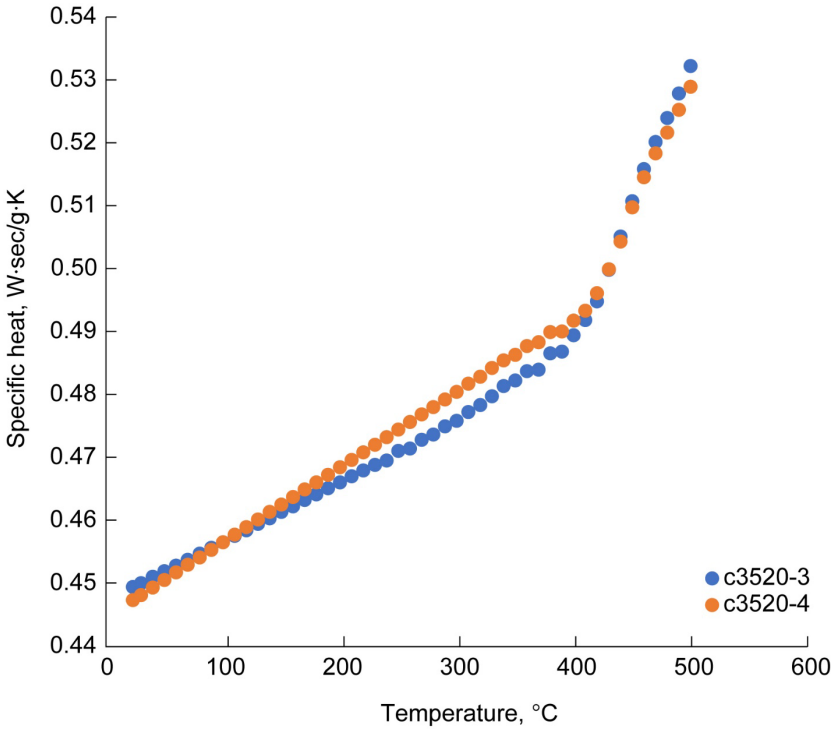

Figure 5.—Specific heat on truncated ordinate axis.

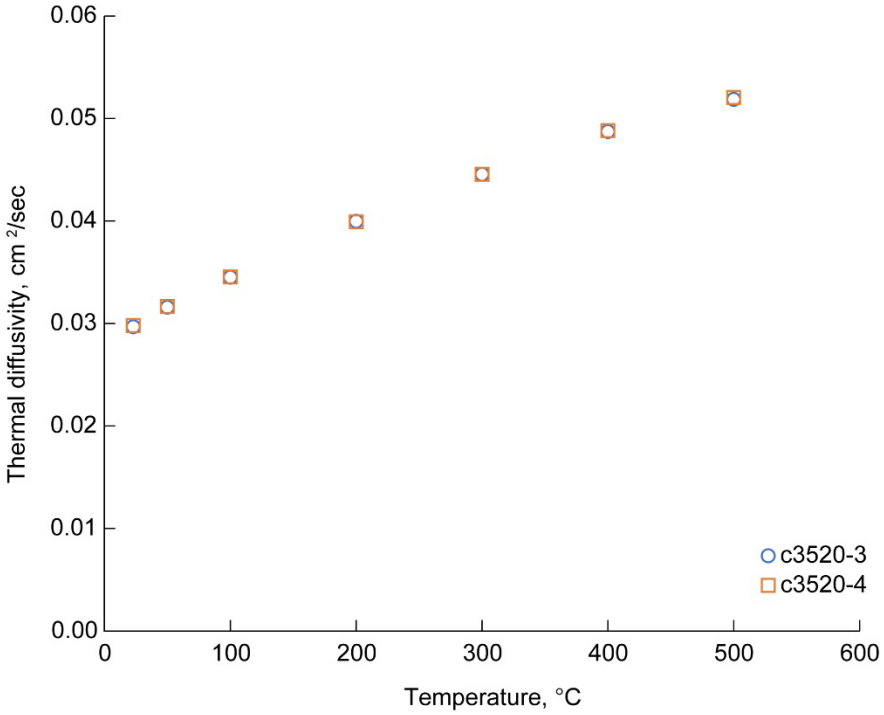

Figure 6.—Thermal diffusivity for the two specimens.

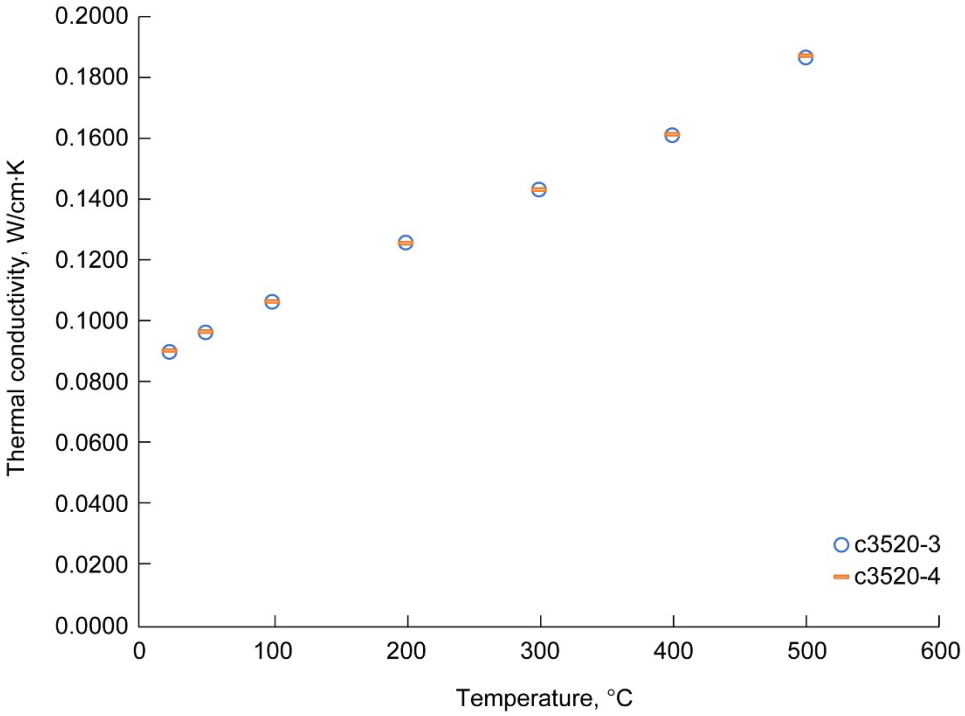

Figure 7.—Thermal conductivity for the studied specimens.

Summary

Selected metallurgical and thermophysical properties of aged Ni-Ti-Hf have been investigated. The average grain size was 90 μm and the average Vickers hardness was 549 HV. Thermophysical properties were measured from room temperature to 500 °C to represent the potential range of operating temperatures. Over the studied temperature range, electrical resistivity increased from approximately 8.9×10^{-7} to 11.3×10^{-7} Ω·m. Thermal expansion coefficients ranged from 1.1×10^{-5} to 1.2×10^{-5} mm/mm·°C. Specific heat ranged from 0.44 to 0.53 W·sec/g·K. Thermal diffusivity increased from approximately 0.003 to 0.005 cm^2/sec. Thermal conductivity rose from approximately 0.09 to 0.19 W/cm·K.

It should be noted that the microstructure of Ni-Ti-Hf is typically refined by hot work. Since the material in this study was heat treated but not subjected to work, further study is needed to characterize the defect structure with respect to thermomechanical work and to determine how the studied properties are affected therewith.

Appendix

Application of the Rule of Mixtures

Using the rule of mixtures for composite materials, certain properties like thermal conductivity, density, and electrical resistivity can be estimated. For example, for electrical resistivity R:

$$R = \sum_i \left(f_i \cdot R_i \right) = f_1 \cdot R_1 + f_2 \cdot R_2 + \ldots + f_n \cdot R_n$$

where $f_1, f_2, \cdots, f_n$ are the volume fractions of each constituent and $R_1, R_2, \cdots, R_n$ are their respective resistivities. Given the following densities of the constituents of 57Ni-40Ti-3Hf (wt%),

$R_{\mathrm{NiTi}} = 9.63\times10^{-7}\ \Omega\cdot\mathrm{m}$
$R_{\mathrm{Hf}} = 3.51\times10^{-7}\ \Omega\cdot\mathrm{m}$

the volume fractions are:

$$\begin{aligned} f_{\mathrm{NiTi}} &= \frac{\mathrm{wt\%NiTi}/R_{\mathrm{NiTi}}}{\mathrm{wt\%NiTi}/R_{\mathrm{NiTi}} + \mathrm{wt\%Hf}/R_{\mathrm{Hf}}} \\ &= \frac{97/9.63\times10^{-7}}{97/9.63\times10^{-7} + 3/3.51\times10^{-7}} \\ &= 0.922 \end{aligned}$$

$$\begin{aligned} f_{\mathrm{Hf}} &= \frac{\mathrm{wt\%Hf}/R_{\mathrm{Hf}}}{\mathrm{wt\%NiTi}/R_{\mathrm{NiTi}} + \mathrm{wt\%Hf}/R_{\mathrm{Hf}}} \\ &= \frac{3/3.51\times10^{-7}}{97/9.63\times10^{-7} + 3/3.51\times10^{-7}} \\ &= 0.078 \end{aligned}$$

$$\begin{aligned} \therefore R &= \sum_i \left(f_i \cdot R_i \right) = \sum \left(f_{\mathrm{NiTi}} \cdot R_{\mathrm{NiTi}} + f_{\mathrm{Hf}} \cdot R_{\mathrm{Hf}} \right) \\ &= 0.922\left(9.63\times10^{-7}\right) + 0.078\left(3.51\times10^{-7}\right) \\ &= 9.15\times10^{-7}\,\Omega\cdot\mathrm{m} \end{aligned}$$

There is a difference of approximately 2 percent in this estimate and the measured value. However, if resistivity were estimated with each element considered as a separate constituent, i.e.:

$$R = \sum \left(f_{\mathrm{Ni}} \cdot R_{\mathrm{Ni}} + f_{\mathrm{Ti}} \cdot R_{\mathrm{Ti}} + f_{\mathrm{Hf}} \cdot R_{\mathrm{Hf}} \right)$$

where

$R_{\mathrm{Ni}} = 8.0\times10^{-7}\ \Omega\cdot\mathrm{m}$
$R_{\mathrm{Ti}} = 4.2\times10^{-7}\ \Omega\cdot\mathrm{m}$
$R_{\mathrm{Hf}} = 3.51\times10^{-7}\ \Omega\cdot\mathrm{m}$

the volume fractions are:

$$f_{\mathrm{Ni}} = \frac{\mathrm{wt\%Ni}/R_{\mathrm{Ni}}}{\mathrm{wt\%Ni}/R_{\mathrm{Ni}} + \mathrm{wt\%Ti}/R_{\mathrm{Ti}} + \mathrm{wt\%Hf}/R_{\mathrm{Hf}}}$$
$$= \frac{57/8.0\times10^{-8}}{57/8\times10^{-8} + 40/4.2\times10^{-7} + 3/3.51\times10^{-7}} = 0.8729$$

$$f_{\mathrm{Ti}} = \frac{40/4.2\times10^{-7}}{57/8\times10^{-8} + 40/4.2\times10^{-7} + 3/3.51\times10^{-7}} = 0.1167$$

$$f_{\mathrm{Hf}} = \frac{3/3.51\times10^{-7}}{57/8\times10^{-8} + 40/4.2\times10^{-7} + 3/3.51\times10^{-7}} = 0.0105$$

$$\therefore R = \sum_i (f_i \cdot R_i) = \sum (f_{\mathrm{Ni}} \cdot R_{\mathrm{Ni}} + f_{Ti} \cdot R_{\mathrm{Ti}} + f_{\mathrm{Hf}} \cdot R_{\mathrm{Hf}})$$
$$= 0.8729\left(8.0\times10^{-8}\right) + 0.01167\left(4.2\times10^{-7}\right) + 0.0105\left(3.51\times10^{-7}\right)$$
$$= 1.22\times10^{-7}$$

The measured value is more than seven times this estimate. So, the rule of mixtures estimate, incorporating NiTi as a single constituent, appears to be a reasonable method for calculation of electrical resistivity of NiTiHf and is more accurate than the solid solution method for the studied material.

For density, performing the calculation with each constituent incorporated separately (this method will hereafter be referred to as the “solid solution technique”) gives us:

$$\rho = \sum_i (f_i \cdot \rho_i) = f_1 \cdot \rho_1 + f_2 \cdot \rho_2 + \ldots + f_n \cdot \rho_n$$

Using the densities of the individual elements:

$\rho_{\mathrm{Ni}} = 8.9\ \mathrm{g/cm^3}$
$\rho_{\mathrm{Ti}} = 4.5\ \mathrm{g/cm^3}$
$\rho_{\mathrm{Hf}} = 13.09\ \mathrm{g/cm^3}$

$$f_{\mathrm{Ni}} = \frac{\frac{57}{8.9}}{\frac{57}{8.9} + \frac{40}{4.5} + \frac{3}{13.09}} = \frac{6.4045}{15.5226} = 0.4126$$

$$f_{\mathrm{Ti}} = \frac{40/4.5}{15.5226} = \frac{8.8889}{15.5226} = 0.5726$$

$$f_{\mathrm{Hf}} = \frac{3/13.09}{15.5226} = \frac{3/13.09}{15.5226} = 0.0148$$

$$\therefore \rho = \sum_i (f_i \cdot \rho_i) = \sum (f_{\mathrm{Ni}} \cdot \rho_{\mathrm{Ni}} + f_{\mathrm{Ti}} \cdot \rho_{\mathrm{Ti}} + f_{\mathrm{Hf}} \cdot \rho_{\mathrm{Hf}})$$
$$= 0.4126(8.9) + 0.5726(4.5) + 0.0148(13.09)$$
$$= 6.44\,\mathrm{g/cm^3}$$

which is within 5 percent of the measured value (6.75 g/cm^3). However, performing the calculation where NiTi is a single constituent, where:

ρ_{NiTi} = 6.66 g/cm^3
ρ_{Hf} = 13.09 g/cm^3

gives us the following volume fractions:

$$f_{\mathrm{Ni}} = \frac{\frac{97.0}{6.66}}{\frac{97.0}{6.66} + \frac{3.0}{13.09}} = \frac{14.564}{14.794} = 0.9845$$

$$f_{\mathrm{Hf}} = \frac{3.0/13.09}{14.794} = 0.0155$$

$$\therefore \rho = \sum_i (f_i \cdot \rho_i) = \sum (f_{\mathrm{NiTi}} \cdot \rho_{\mathrm{NiTi}} + f_{\mathrm{Hf}} \cdot \rho_{\mathrm{Hf}})$$
$$= 0.9845(6.66) + 0.0155(13.09) = 6.76\,\mathrm{g/cm^3}$$

which is within 0.2 percent of the measured value. Therefore, the rule of mixtures method is more accurate than the solid solution method for 57Ni-40Ti-3Hf (wt%).

Similarly, to estimate thermal conductivity using the solid solution technique:

$$\kappa = \sum_i (f_i \cdot \kappa_i) = f_1 \cdot \kappa_1 + f_2 \cdot \kappa_2 + \ldots + f_n \cdot \kappa_n$$

using the following densities of the individual elements:

κ_{Ni} = 92
κ_{Ti} = 22
κ_{Hf} = 22.3

yields the following volume fractions:

$$f_{\mathrm{Ni}} = \frac{\frac{57}{92}}{\frac{57}{92} + \frac{40}{22} + \frac{3}{22.3}} = \frac{0.6196}{2.5723} = 0.2409$$

$$f_{\mathrm{Ti}} = \frac{40/22}{2.5723} = \frac{1.8182}{2.5723} = 0.7068$$

$$f_{\mathrm{Hf}} = \frac{3/22.3}{2.5723} = \frac{0.1345}{2.5723} = 0.0523$$

$$\therefore \kappa = \sum \left(f_{\mathrm{Ni}} \cdot \kappa_{\mathrm{Ni}} + f_{\mathrm{Ti}} \cdot \kappa_{\mathrm{Ti}} + f_{\mathrm{Hf}} \cdot \kappa_{\mathrm{Hf}} \right)$$

$$= 0.2409(92) + 0.7068(22) + 0.0523(22.3)$$

$$= 38.9\ \mathrm{W/m \cdot K}$$

which is more than four times the measured value (8.9 W/m·K). However, performing the calculation where NiTi is a single constituent, where:

κ_{NiTi} = 8.9 W/m·K
κ_{Hf} = 22.3 W/m·K

gives us the following volume fractions:

$$f_{\mathrm{NiTi}} = \frac{\frac{97}{8.9}}{\frac{97}{8.9} + \frac{3.0}{22.3}} = \frac{10.90}{4.484} = 0.988$$

$$f_{\mathrm{Hf}} = \frac{3.0/22.3}{4.484} = 0.0122$$

$$\therefore \kappa = \sum \left(f_{\mathrm{NiTi}} \cdot \kappa_{\mathrm{NiTi}} + f_{\mathrm{Hf}} \cdot \kappa_{\mathrm{Hf}} \right)$$

$$= 0.9845(8.9) + 0.030(22.3) = 9.06\ \mathrm{W/m \cdot K}$$

which is within 8 percent of the measured value (9.8 W/m·K). So, the rule of mixtures could be used as a first approximation of thermal conductivity for the studied material, especially compared to the solid solution technique.

References

1. C. DellaCorte, S.V. Pepper, R.D. Noebe, D.R. Hull and G. Glennon, Intermetallic Nickel-Titanium Alloys for Oil-Lubrication Bearing Applications, NASA/TM—2009-215646, March 2009.
2. S.V. Pepper, C. DellaCorte, R.D. Noebe, D.R. Hull and G. Glennon, Nitinol 60 as a Material for Spacecraft Triboelements, ESMATS 13 Conference, Vienna, Austria, September 2009.
3. M.K. Stanford, "Hardness and Microstructure of Binary and Ternary Nitinol Compounds," NASA/TM—2016-218946/REV1, December 2019.
4. M.K. Stanford, "Thermophysical Properties of 60-Nitinol for Mechanical Component Applications," NASA/TM—2012-216056, December 2012.
5. R. Larsen, T. Goerz and C. Crochet, "Thermophysical Properties of Two Samples," TPRL Report Number 6021, Thermophysical Properties Research Laboratory, Inc., West Lafayette, IN, 2022.
6. ASTM E112-10, 2001, "Standard Test Method for Determining Average Grain Size," vol. 03.01, ASTM Standards, vol. 14.02, American Society for Testing and Materials, West Conshohocken, PA.
7. ASTM E384-11, 2011, Standard Test Method for Knoop and Vickers Hardness of Materials," ASTM Standards, vol. 03.01, American Society for Testing and Materials, West Conshohocken, PA.
8. I. Miccoli, F. Edler, H. Pfnür and C. Tegenkamp, "The 100th anniversary of the four-point probe technique: the role of probe geometries in isotropic and anisotropic systems," 2015, Journal of Physics: Condensed Matter, vol. 27, no. 22.
9. ASTM E228-17, Standard Test Method for Linear Thermal Expansion of Solid Materials with a Push-Rod Dilatometer, ASTM Standards, 2012, ASTM Standards, vol. 14.02, American Society for Testing and Materials, West Conshohocken, PA.
10. ASTM 1269-11, Standard Test Method for Determining Specific Heat Capacity by Differential Scanning Calorimetry, ASTM Standards, vol. 14.01, American Society for Testing and Materials, West Conshohocken, PA.
11. ASTM E1461-13, Standard Test Method for Thermal Diffusivity by the Flash Method, ASTM Standards, vol. 14.01, American Society for Testing and Materials, West Conshohocken, PA.
12. M.K. Stanford, A. Garg, R.B. Rogers, "Microstructure and Hardness of 57Ni – 40Ti – 3Hf (wt%)," NASA/TM-20205003290, August 2020.
13. P.G. Klemens, "Theory of Thermal Conductivity, R.P. Tye, ed., Academic Press, London, 1969, pp. 1–68.
14. M. Braunović, "Electrical and Electronic Behavior," in Intermetallic Compounds: Magnetic, Electrical and Optical Properties and Applications of Intermetallic Compounds, J.H. Westbrook and R.L. Fleischer eds., John Wiley & Sons Ltd., West Sussex, England, 2000.
15. G. Grimvall, "Thermophysical Properties of Materials," enlarged and revised edition, Elsevier Science, Amsterdam, 1999.